Biochemical and Biophysical Research Communications 442 (2013) 8–15

Contents lists available at ScienceDirect

Biochemical and Biophysical Research Communications

journal homepage: www.elsevier.com/locate/ybbrc

Cold stress accentuates pressure overload-induced cardiac hypertrophy and contractile dysfunction: Role of TRPV1/AMPK-mediated autophagy

Songhe Lu, Dezhong Xu *

Department of Epidemiology, The Fourth Military Medical University, 127 West Changle Road, Xi'an, Shaanxi 710032, PR China

ARTICLE INFO

Article history:
Received 22 October 2013
Available online 5 November 2013

Keywords:
Cold exposure
Mitochondrial
Pressure overload
Heart failure
Autophagy

ABSTRACT

Severe cold exposure and pressure overload are both known to prompt oxidative stress and pathological alterations in the heart although the interplay between the two remains elusive. Transient receptor potential vanilloid 1 (TRPV1) is a nonselective cation channel activated in response to a variety of exogenous and endogenous physical and chemical stimuli including heat and capsaicin. The aim of this study was to examine the impact of cold exposure on pressure overload-induced cardiac pathological changes and the mechanism involved. Adult male C57 mice were subjected to abdominal aortic constriction (AAC) prior to exposure to cold temperature (4 °C) for 4 weeks. Cardiac geometry and function, levels of TRPV1, mitochondrial, and autophagy-associated proteins including AMPK, mTOR, LC3B, and P62 were evaluated. Sustained cold stress triggered cardiac hypertrophy, compromised depressed myocardial contractile capacity including lessened fractional shortening, peak shortening, and maximal velocity of shortening/relengthening, enhanced ROS production, and mitochondrial injury, the effects of which were negated by the TRPV1 antagonist SB366791. Western blot analysis revealed upregulated TRPV1 level and AMPK phosphorylation, enhanced ratio of LC3II/LC3I, and downregulated P62 following cold exposure. Cold exposure significantly augmented AAC-induced changes in TRPV1, phosphorylation of AMPK, LC3 isoform switch, and p62, the effects of which were negated by SB366791. In summary, these data suggest that cold exposure accentuates pressure overload-induced cardiac hypertrophy and contractile defect possibly through a TRPV1 and autophagy-dependent mechanism.

1. Introduction

Epidemiologic studies have indicated that exposure to low ambient temperature may lead to compromised cardiovascular health and/or precipitate cardiovascular events. In 1999, a group of French scientists reported a winter peak in hospitalizations and death in heart failure (HF) for the first time [1]. Over the following two decades, the same phenomenon was observed all over the world [2–6]. Several mechanisms have been postulated to contribute to the cold weather-associated aggravation of heart failure. In particular, exposure to cold climate may facilitate sympathetic over-activation. In consequence, vasoconstriction develops in association with higher afterload, increase of blood pressure [7] and a decline in cardiac output in subjects living in cold climate [8]. Nonetheless, the precise cellular mechanism responsible for the higher prevalence of heart failure under cold stress remains essentially elusive.

Transient receptor potential vanilloid 1 (TRPV1) is considered as an accessory of the breakthrough in the field of somatic sensory biology and pain research [9]. As a nonselective cation channel, TRPV1 may be activated by a wide variety of exogenous and endogenous physical and chemical stimuli. Among which, heat and capsaicin are perhaps two best-known activators [9,10]. Further studies revealed that functional TRPV1 channels are located in the central nervous system [11,12] and non-neuronal tissues including epidermal keratinocytes of human skin [13], human bronchial fibroblast [14] and cardiovascular system [15,16]. Moreover TRPV1 is reported to play a key role in not only pain and temperature sensation but also many other physiological or pathophysiological processes. With the identification for TRPV1 localization in left ventricles, the importance of this channel in the regulation of heart function has drawn much attention recently [17–19]. For example, increased TRPV1 channel expression was observed in hypertrophic hearts [20]. Mice lacking functional TRPV1 are found to be protected against pressure overload-induced cardiac hypertrophy [16]. Coincidentally, TRPV1 antagonists are deemed effective in the management of cardiac hypertrophy and heart failure [21]. More recent evidence indicated that TRPV1 facilitates autophagy in a ROS- and AMPK-dependent manner [22]. Not surprisingly, cardiac hypertrophy was to be concomitant with an increase in autophagosomes and mitochondrial biogenesis, in an effort to replenish the damaged mitochondria and to restore energy production. As a major site of free radical production in the

* Corresponding author.
E-mail address: dezhongxu@126.com (D. Xu).

0006-291X/$ - see front matter © 2013 Published by Elsevier Inc.
http://dx.doi.org/10.1016/j.bbrc.2013.10.128

face of oxidative phosphorylation, mitochondria are believed to be the primary target for oxidative damage under stress [23]. To this end, this study was designed to examine the impact of cold exposure on pressure overload-induced cardiac pathological changes and the underlying mechanisms involved. Given the pivotal role of temperature sensor TRPV1 in the onset and development of cardiac hypertrophy, special focus was made towards TRPV1 and subsequently autophagy in the interplay between cold stress and pressure overload in the heart.

2. Materials and methods

2.1. Experimental design and abdominal aortic constriction (AAC) surgery

All animal procedures used in this study were approved by the Animal Care and Use Committee at the Fourth Military Medical University (Xi'an, China). In brief, one hundred and fifty 12- to 16-week-old adult male C57BL6 mice were randomly divided into five groups: (1) Normal temperature + sham (NT-S); (2) Low temperature + sham (LT-S); (3) Normal temperature + AAC (NT-AAC); (4) Low temperature + AAC (LT-AAC); (5) Low temperature + AAC + SB366791 (LT-AAC-SB, 500 μg/kg, i.p.) [24]. Mice were anesthetized (phenobarbital sodium, 50 mg/kg, i.p.) and were placed in a supine position prior to the AAC or sham procedure. Abdomen was opened under sterilize conditions and abdominal aorta were dissected free at the suprarenal level of surrounding adventitial adipose tissues and muscles. A 6-0 silk suture was tied around the abdominal aorta between celiac and superior mesenteric arteries and a blunted 29-gauge needle to yield a ~33% narrowing of luminal diameter. Sham operation included all surgical procedures except the suture ligation.

2.2. Cold exposure and drug treatment

Mice were housed at room temperature or low temperature in a cold room (4 °C) with free access to food and water for 4 weeks after sham or AAC surgery. Systolic and diastolic blood pressures were evaluated using a semi-automated, amplified tail cuff device. Myocardial morphology and function were examined. A cohort of mice were subject to cold temperature for 4 weeks while receiving the selective TRPV1 receptor antagonist SB366791 (500 μg/kg, i.p., Sigma Aldrich, Louis, MO, USA) or 0.2% dimethylsulfoxide (DMSO) vehicle prior to the AAC surgery [25].

2.3. Echocardiographic assessment

Cardiac geometry and function were evaluated in anesthetized (Avertin 2.5%, 10 μl/g body weight, i.p.) mice using the 2-D guided M-mode echocardiography (Sonos 5500) equipped with a 15 MHz linear transducer. Left ventricular (LV) anterior and posterior wall dimensions during diastole and systole were recorded from three consecutive cycles in M-mode using methods adopted by the American Society of Echocardiography. Fractional shortening was calculated from LV end-diastolic (EDD) and end-systolic (ESD) diameters using the equation (EDD-ESD)/EDD [26].

2.4. Isolation of murine cardiomyocytes and Cell shortening/relengthening

After ketamine/xylazine sedation (ketamine 80 mg/kg and xylazine 12 mg/kg, i.p.), hearts were removed and perfused with Krebs-Henseleit bicarbonate (KHB) buffer at room temperature containing (in mM): 118 NaCl, 4.7 KCl, 1.2 $MgSO_4$, 1.2 KH_2PO_4, 25 $NaHCO_3$, 10 HEPES, and 11.1 glucose. Hearts were digested with collagenase D for 20 min. Left ventricles were removed and minced before being filtered. Mechanical properties of rod-shaped cardiomyocytes were assessed using an IonOptix™ soft-edge system (IonOptix, Milton, MA, USA). Myocytes were field stimulated at 0.5 Hz. Cell shortening and relengthening were assessed including peak shortening (PS), time-to-PS (TPS), time-to-90% relengthening (TR_{90}) and maximal velocities of shortening/relengthening (±dL/dt) [27].

2.5. Histological examination

Following anesthesia, hearts were excised and immediately placed in 4% paraformaldehyde at room temperature for 24 h. The myocardial specimen were embedded in paraffin, cut in 5 μm sections and stained with hematoxylin and eosin (H&E) as well as FITC-conjugated wheat germ agglutinin. Cardiomyocyte cross-sectional areas were calculated on a digital microscope (×400) using the Image J (version 1.34S) software [26,28].

2.6. Western blot analysis

Proteins were prepared as described [26]. Samples containing equal amount of proteins were separated on 10% SDS–polyacrylamide gels in a minigel apparatus (Mini-PROTEAN II, Bio-Rad) and transferred to nitrocellulose membranes. The membranes were blocked with 5% milk in TBS-T, and were incubated overnight at 4 °C with anti-TRPV1, anti-AMPKα, anti-pAMPKα (Thr172), anti-mTOR, anti-pmTOR (Ser2448), anti-P62 anti-LC3B antibodies. After immunoblotting, the film was scanned and the intensity of gel bands was detected using a Bio-Rad Calibrated Densitometer. GAPDH was used as the loading control. Protein levels of TRPV1, AMPK, mTOR, P62, and LC3B were determined in left ventricular tissues 30 days following AAC or sham surgery.

Table 1
Biometric parameters of C57 mice in normal or cold exposure after AAC and sham surgery.

Parameter	NT-sham	NT-AAC	LT-sham	LT-AAC	LT-AAC-SB
Body weight (g)	25.5 ± 1.3	25.2 ± 0.9	26.3 ± 1.2	24.9 ± 0.6	24.8 ± 1.2
Heart weight (mg)	152 ± 5	179 ± 6*	153 ± 7	188 ± 4*#	162 ± 8$
Heart/body weight ratio (mg/g)	5.96 ± 0.15	7.10 ± 0.32*	5.82 ± 0.12	7.55 ± 0.21*#	6.53 ± 0.11$
Liver weight (g)	1.62 ± 0.09	1.59 ± 0.08	1.65 ± 0.10	1.53 ± 0.06	1.55 ± 0.05
Liver/body weight (mg/g)	63.5 ± 2.3	63.1 ± 1.9	62.7 ± 1.5	61.4 ± 2.1	65.7 ± 1.8
Kidney weight (g)	0.48 ± 0.03	0.42 ± 0.06	0.51 ± 0.05	0.44 ± 0.06	0.46 ± 0.07
Kidney/body weight (mg/g)	18.8 ± 0.5	16.7 ± 0.7	19.4 ± 0.7	17.7 ± 0.6	19.5 ± 0.7
EDD (mm)	2.53 ± 0.09	2.92 ± 0.10*	2.56 ± 0.11	3.30 ± 0.12*#	2.93 ± 0.11$
ESD (mm)	1.32 ± 0.11	1.86 ± 0.12*	1.23 ± 0.13	2.20 ± 0.11*#	1.79 ± 0.11$
FS (%)	55.2 ± 2.9	39.6 ± 1.6*	48.6 ± 2.1	26.3 ± 1.9*#	40.6 ± 1.1$

EDD = end diastolic diameters; ESD = end systolic diameters; FS = fractional shortening; Mean ± SEM, n = 13–14 mice per group.
* $p < 0.05$ vs. NT-sham group.
# $p < 0.05$ vs. NT-AAC group.
$ $p < 0.05$ vs. LT-AAC group.

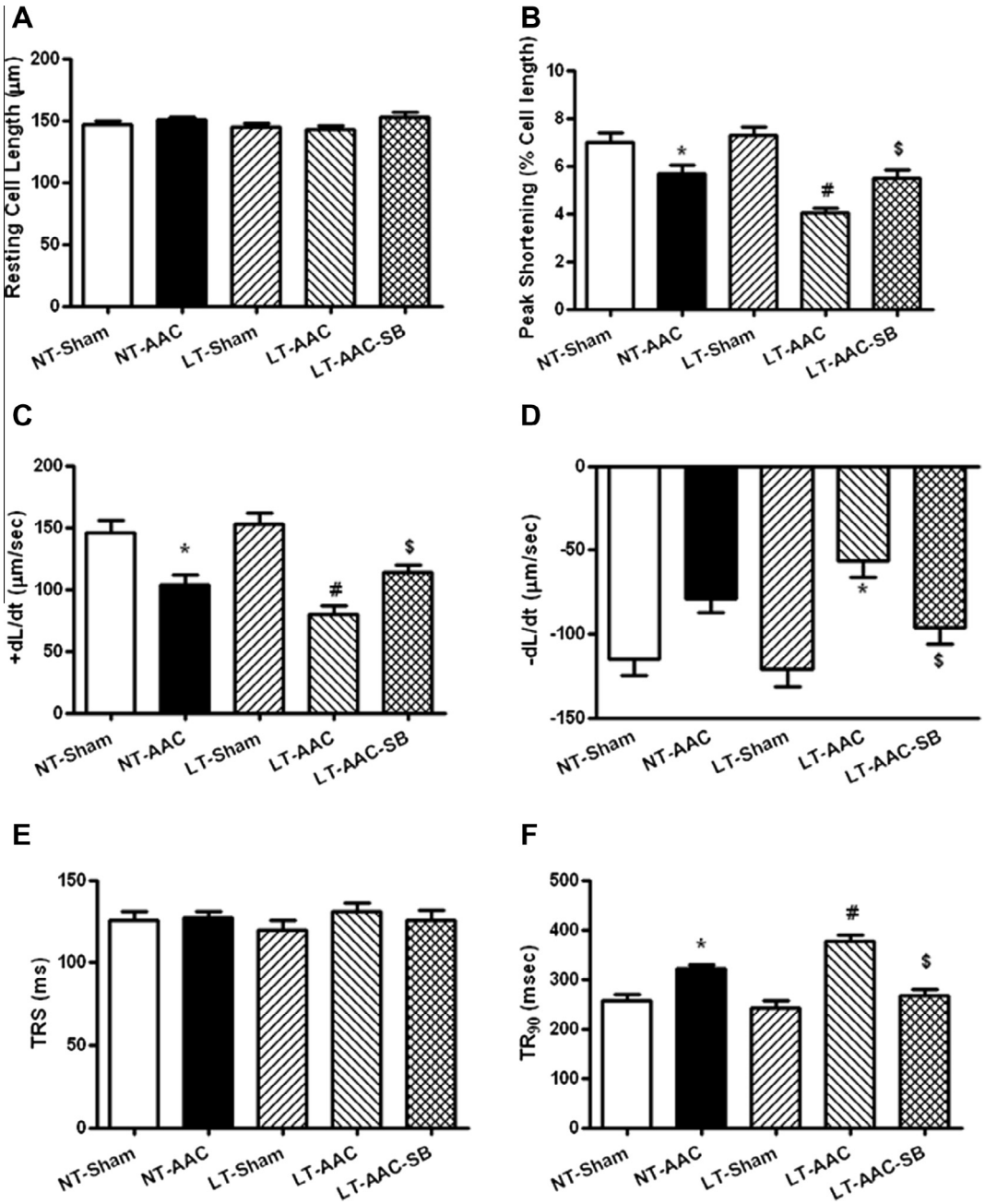

Fig. 1. Contractile properties of cardiomyocytes from LT and NT treated mouse hearts following AAC or sham surgery. (A) resting cell length; (B) peak shortening (normalized to cell length) (C) maximal velocity of shortening (+dL/dt); (D) maximal velocity of relengthening (−dL/dt); (E) Time-to-PS (TPS); and (F) Time-to-90% relengthening (TR_{90}). Mean ± SEM, n = 100 cells from 3 to 5 mice/group, $^{*}p < 0.05$ vs. NT-sham group, $^{\#}p < 0.05$ vs. NT-AAC group, $^{\$}p < 0.05$ vs. LT-AAC group.

2.7. Measurement of mitochondrial membrane potential (MMP)

Cardiomyocytes were suspended in HEPES-saline buffer and mitochondrial membrane potential ($\Delta\Psi_m$) was detected as described [29]. Briefly, after pre-incubation with 5 μM JC-1 for 10 min at 37 °C, cells were washed two times by sedimentation using HS buffer free of JC-1 and resuspended in MEM supplemented with MG-AGE or BSA (2.5 μmol/l) at 37 °C for 4 h. During the incubation period, cardiomyocytes were examined periodically under confocal laser scanning microscope (Leica TCS SP2) at excitation wavelength of 490 nm and emission fluorescence was recorded at 530 nm (monomer form of JC-1, green) and at 590 nm (aggregate form of JC-1, red). Alternatively, fluorescence of each sample was read at excitation wavelength of 490 nm and emission wavelength of 530 nm and 590 nm using a spectrofluorimeter (Spectra MaxGeminiXS) at an interval of 10 s. Results in fluorescence intensity were expressed as 590–530 nm emission ratio.

2.8. Generation of intracellular reactive oxygen species (ROS)

Production of ROS was evaluated by changes in the fluorescence intensity resulted from oxidation of the intracellular fluoroprobe 5-(and -6)-chloromethyl-2′,7′-dichlorodihydrofluorescein diacetate (CM-H2-DCF-DA, Molecular Probes, Eugene, OR, USA). In brief, cardiomyocytes were incubated with 25 μM CM-H2DCF-DA for 30 min at 37 °C. Cells were rinsed before fluorescence intensity was measured using a fluorescent micro-plate reader at the excitation and emission wavelengths of 480 and 530 nm, respectively (Molecular Devices, Sunnyvale, CA, USA). Untreated cells without

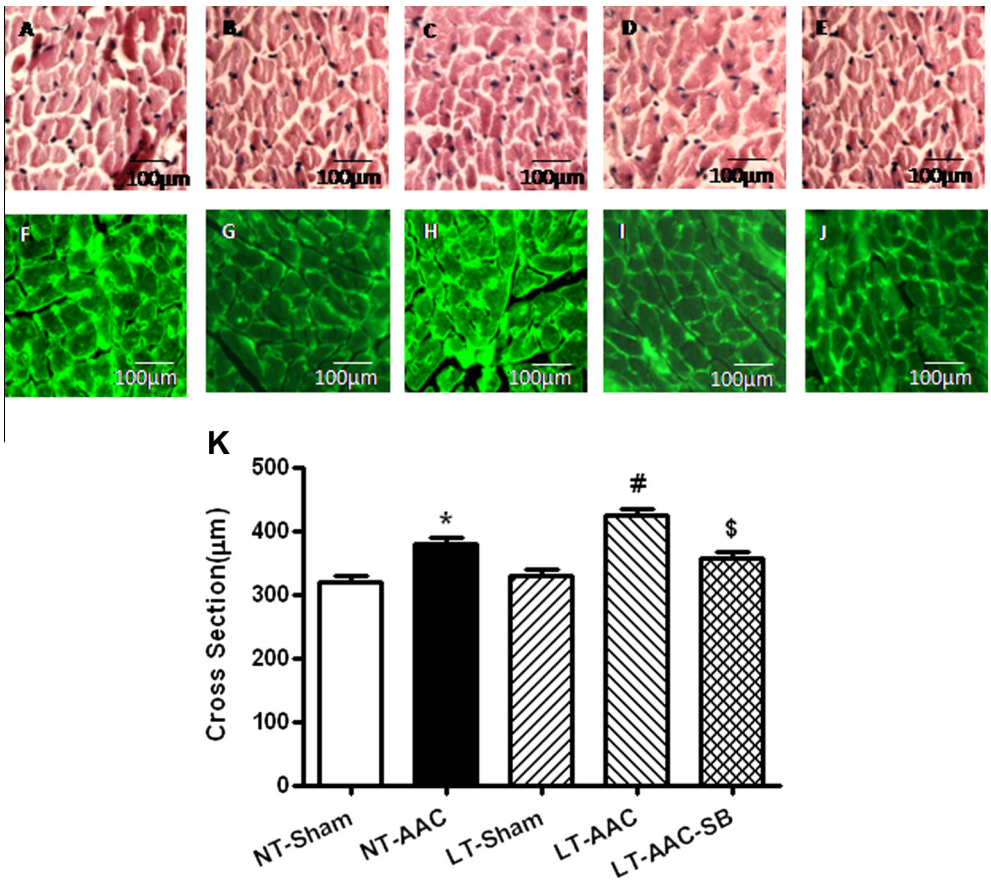

Fig. 2. Effects of cold exposure on AAC-induced cardiac hypertrophy using H&E and FITC-conjugated staining. H&E staining transverse sections of left ventricular myocardium (×400) in panels (A) (NT-sham), (B) (NT-AAC), (C) (LT-sham), (D) (LT-AAC) and (E) (LT-AAC-SB). FITC-conjugated Lectin immunostaining depicting transverse sections of left ventricular myocardium in panels (F) (NT-sham), (G) (NT-AAC), (H) (LT-sham), (I) (LT-AAC) and (J) (LT-AAC-SB). Original magnification = 400×. (K) quantitative analysis of cardiomyocyte cross-sectional area. Mean ± SEM, n = 15 and 10 fields from 4 to 5 mice per group for panel K, $^{*}p < 0.05$ vs. NT-sham group, $^{\#}p < 0.05$ vs. NT-AAC group, $^{\$}p < 0.05$ vs. LT-AAC group.

fluorescence were used as the background fluorescence. The final results were expressed as the ratio of the fluorescent intensity normalized to respective protein content [30].

2.9. Data analysis

Data were mean ± SEM. Statistical significance ($p < 0.05$) for each variable was estimated by analysis of one-way variance (ANOVA) followed by a Tukey's *post hoc* analysis.

3. Results

3.1. General biometric and echocardiographic properties of C57 mice after AAC in cold exposure

Neither cold exposure nor AAC surgery overtly affected body, heart, liver, and kidney weights or sizes (liver and kidney) (Table 1). AAC procedure but not cold stress significantly increased cardiac size (normalized to body weight) with a more pronounced effect with the combination of the two. AAC procedure but not cold stress significantly enlarged LV EDD and LV ESD as well as decreased fractional shortening, with a more pronounced response with concomitant cold stress and pressure overload. Interestingly, the TRPV1 antagonist SB366791 effectively reconciled cold stress-induced accentuation of cardiac hypertrophy and echocardiographic changes without affecting the size of liver and kidney following pressure overload. These data indicated that cold stress is capable of aggravating pressure overload-induced cardiac geometric and functional anomalies, the effect of which may be mitigated by the TRPV1 antagonist SB366791.

3.2. Effects of cold exposure and TRPV1 antagonism on AAC-induced cardiomyocyte contractile dysfunction

To evaluate the effect of cold exposure on pressure overload-induced cardiomyocyte contractile function, mechanical property of isolated cardiomyocytes was assessed in sham or AAC-operated mice under normal temperature or cold stress. The resting cell length was comparable among sham or AAC group under normal or cold environment. As expected, AAC procedure significantly reduced PS, ±dL/dt, and prolonged TR_{90} without affecting TPS. Although cold stress itself did not affect cardiomyocyte mechanical parameters, it significantly attenuated or abrogated AAC-induced cardiomyocyte mechanical defects (Fig. 1). Interestingly, cold stress-induced accentuation of AAC-induced cardiomyocyte anomalies was nullified by the TRPV1 antagonist SB366791.

3.3. Effects of cold exposure and TRPV1 antagonism on AAC-induced cardiac hypertrophy

To further assess the impact of cold stress on AAC-induced myocardial hypertrophy, cardiomyocyte cross-sectional area was monitored. Data from H&E and FITC-conjugated wheat germ agglutinin staining revealed that cold exposure overtly increased

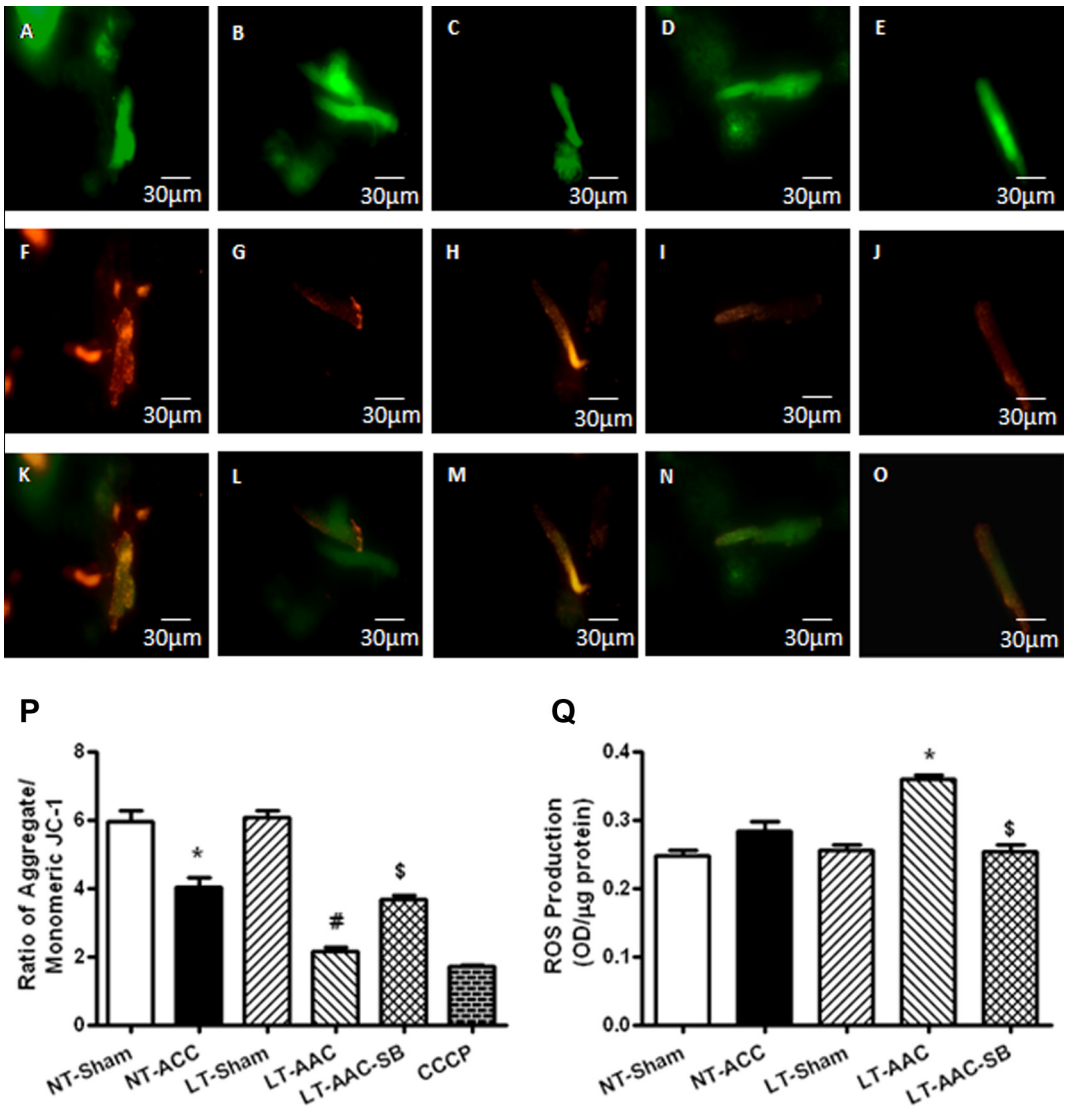

Fig. 3. Effects of cold exposure on AAC induced change of mitochondrial membrane potential and ROS generation. Representative images of JC-1 staining of cardiomyocytes (A–L) scale bar = 30 μm). (A–E) monomeric JC-1; (F and J) aggregate JC-1; (K–O) merged figures: (A, F, K) NT-sham; (B, G, L) NT-AAC; (C, H, M) LT-sham; (D, I, N) LT-AAC; (E, J, O) LT-AAC-SB. (P) Quantitative analysis of the red/ green fluorescence ratio (~50 cardiomyocytes from 5 mice per group). (Q) ROS production measured by DCFfluorescence. Mean ± SEM, $n = 50$ cardiomyocytes from 4 to 5 mice per group, $^{*}p < 0.05$ vs. NT-sham group, $^{\#}p < 0.05$ vs. NT-AAC group, $^{\$}p < 0.05$ vs. LT-AAC group. (For interpretation of reference to colour in this figure legend, the reader is referred to the web version of this article.)

AAC-induced enlargement of cardiomyocyte transverse cross-sectional area without eliciting any effect itself, consistent with the increased left ventricular mass and heart weight. Intriguingly, the TRPV1 antagonist SB366791 effectively abrogated cold stress-exacerbated cardiomyocyte hypertrophy under pressure overload (Fig. 2).

3.4. Effects of cold exposure on AAC-induced change of mitochondrial membrane potential and ROS generation

To examine the potential mechanism(s) of action behind the cold stress and TRPV1 antagonism-elicited effects in cardiac geometry and contractile function following AAC surgery, ROS generation, and mitochondrial membrane potential (using JC-1) were examined in cardiomyocytes from cold stress- and/or AAC-treated mice. Results in Fig. 3 depict that LT-AAC group displayed significantly pronounced DCF staining in conjunction with decreased levels of JC-1 compared with NT-AAC group. The TRPV1 antagonist SB366791 effectively restored the levels of ROS and JC-1. These results indicate that generation of ROS and mitochondrial integrity were significantly altered in cardiomyocytes from pressure overloaded mice, with a more pronounced response under cold stress. Consistent with its mechanical and morphometric responses, SB366791 obliterated or significantly ameliorated cold exposure-induced ROS generation and mitochondrial injury. Cold exposure itself exerted minimal effects on ROS generation and mitochondrial integrity in the absence of cold stress.

3.5. Western blot analysis of TRPV1, activation of AMPK, mTOR and autophagy markers

To further elucidate the potential mechanism(s) involved in cold stress- and/or TRPV1 antagonism-elicited cardiac geometric and functional changes under pressure overload, we went onto examine the expression of the temperature sensor TRPV1 and its downstream signaling molecules including AMPK and mTOR. Given that AMPK and mTOR are two key regulators of autophagy, protein markers for autophagy including p62 and LC3II were also

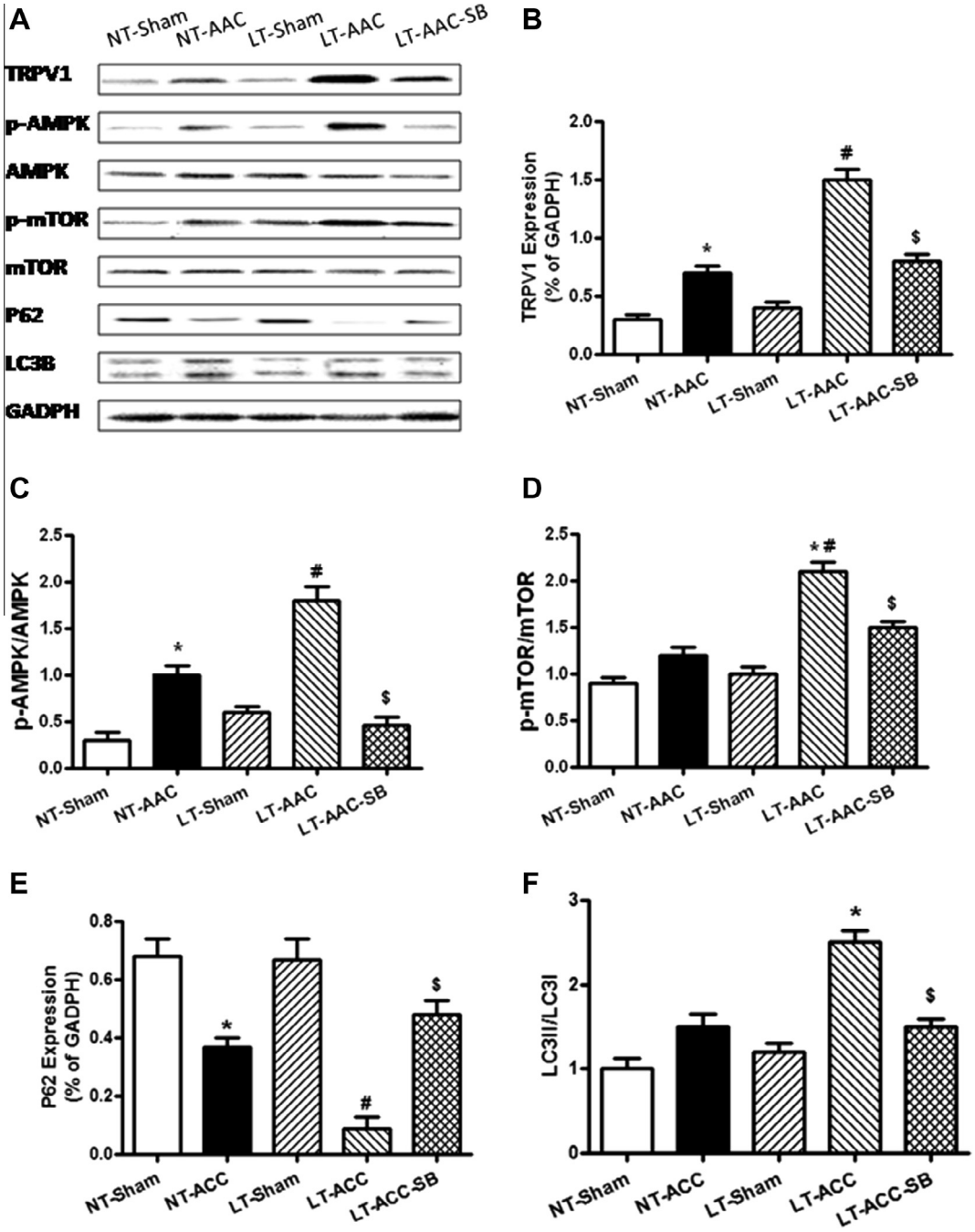

Fig. 4. Western blot analysis of TRPV1, activation of AMPK, mTOR and autophgy markers including p62 and LC3B. (A) representative gel blots of TRPV1, pAMPK, AMPK, pmTOR, mTOR, PGC1α, p62, and LC3B and GAPDH (loading control) using specific antibodies; (B) TRPV1; (C) pAMPK, AMPK; (D) pmTOR, mTOR; (E) p62; and (F) LC3II/LC3I. All proteins were normalized to the loading control GAPDH. Mean ± SEM, $n = 8–9$ mice per group, $^{*}p < 0.05$ vs. NT-sham group, $^{\#}p < 0.05$ vs. NT-AAC group, $^{\$}p < 0.05$ vs. LT-AAC group.

monitored. As shown in Fig. 4, AAC surgery led to upregulated TRPV1 expression, AMPK phosphorylation, downregulated P62 and enhanced ratio of LC3II/LC3I, without affecting the phosphorylation of mTOR. Although cold exposure itself failed to affect these proteins or signaling markers of autophagy, it significantly augmented AAC-induced changes in TRPV1, phosphorylation of AMPK, and mTOR, LC3 isozyme switch and p62. SB366791 effectively reversed cold stress-induced deterioration in these proteins. Total protein expression of AMPK and mTOR was unaffected by either cold exposure or AAC procedure.

4. Discussion

The salient findings from our present study demonstrated that cold exposure significantly accentuated pressure overload-induced cardiac geometric and contractile dysfunction. Our data further revealed that sustained cold exposure significantly augmented pressure overload-induced generation of ROS and mitochondrial injury, upregulation of the temperature sensor protein TRPV1, and downregulation of p62, indicating a likely role of TRPV1 and autophagy in cold stress-induced exacerbation of cardiac contractile and geo-

metric anomalies. Our observation further depicted that cold exposure-induced changes in cardiac contractile and geometric defects under pressure overload may be effectively rescued by the TRPV1 antagonist SB366791. Our findings supported a pivotal role of TRPV1 in cold exposure-induced accentuation of pressure overload-induced cardiac hypertrophic and contractile anomalies. These data support the notion of the TRPV1-AMPK signaling cascade and upregulated autophagy in the pathogenesis of cold stress-induced exacerbation of myocardial anomalies in response to pressure overload. These findings suggest the likely therapeutic potential of TRPV1 antagonism and autophagy in pressure overload-induced myocardial anomalies under cold exposure.

Cold exposure, if sustained, decreased plasma nitric oxide (NO) levels and cardiac antioxidant capacity, while promoting ROS production and apoptosis [31]. Our present study revealed that cold exposure for a duration of 4 weeks exacerbated pressure overload-induced cardiac hypertrophy and contractile dysfunction. The capability of ROS accumulation to facilitate myocardial hypertrophy under pressure overload is somewhat consistent with our current findings of enlarged cardiomyocyte size and hypertrophied heart following cold stress. These findings clearly indicated a role of oxidative stress in cold stress-induced exacerbation of cardiac injury. Results from immunoblotting analysis indicated that cold exposure-induced exacerbation of cardiac hypertrophic and contractile changes following pressure overload were associated with the enhanced myocardial autophagy. Our data further exhibited that cold stress augmented cardiac remodeling following pressure overload as evidenced by heart weight, heart size, left ventricular wall thickness, and histological changes. Our observation that cold stress augmented AAC-induced TRPV1, AMPK phosphorylation, and downregulated P62 expression in the face of pressure overload further suggested a possible role of the TRPV1-AMPK driven facilitation of autophagy in the regulation of cardiac hypertrophy.

Perhaps the most interesting findings from our study were that cold stress augmented pressure overload-induced upregulation of TRPV1 and subsequently AMPK activation along with upregulated autophagy. This is in concert with the findings that TRPV1 antagonist rescued against cold stress-induced exacerbation of cardiac geometric and functional defects under pressure overload. It is likely that TRPV1 governs the AMPK-dependent autophagy *en route* to cardiac remodeling under cold stress and/or pressure overload. TRPV1 as a six trans-membrane tetrameric nonselective cation channel is typically associated with peripheral sensory neurons involved in nociception and baroreflex responses [9]. In addition to the peripheral sensory neurons, TRPV1 is also widely distributed in the heart and circulatory system including cardiomyocytes, blood vessels, pulmonary artery smooth muscle cells, and coronary endothelial cells. TRPV1 expression is upregulated in hypertrophic and myocardial infarction-remodeled hearts [16,32]. Given that TRPV1 antagonism rescued against cold stress-induced contractile defects in response to pressure overload, our data support a TRPV1-mediated mechanism in the regulation of cardiac homeostasis under cold stress and/or pressure overload. Our data revealed that cold exposure accentuates pressure overload-induced mitochondrial injury as evidenced by loss of mitochondrial membrane potential (MMP), an indicator for mitochondrial integrity [33]. Further study is warranted to better elucidate the precise mechanism behind TRPV1-engaged regulation on mitochondrial integrity, autophagy and contractile function in the heart under concomitant cold stress and pressure overload.

Our current study suggested that cold stress-induced phosphorylation of AMPK may underscore facilitated autophagy under pressure overload. Although the precise mechanism of action cannot be offered at this time, it may be speculated that cold stress-promoted ROS production under pressure overload may contribute to cold stress-induced regulation of AMPK activation [34]. It is noteworthy that the natural TRPV1 ligand capsaicin is capable of activating the cellular fuel signal molecule AMPK [22]. Thus upregulated TRPV1 expression under cold stress with concomitant pressure overload may drastically promote excessive autophagy.

In summary, our present study provides evidence, for the first time, that cold tress accentuated pressure overload-induced cardiac hypertrophy and contractile anomalies. Our data indicated that TRPV1, oxidative stress, and AMPK overactivation associated excessive autophagy are involved in mitochondrial damage and cardiac pathology in cold stress- and pressure overload-elicited changes in cardiac anomalies. Our further study using the TRPV1 antagonist consolidated a therapeutic potential of TRPV1 as a target in cold stress-associated myocardial comorbidities, in particular with concomitant pressure overload.

Acknowledgments

This work was supported by research Grants from Natural Science Foundation of China (Grant Number 81200102).

References

[1] F. Boulay, F. Berthier, O. Sisteron, Y. Gendreike, P. Gibelin, Seasonal variation in chronic heart failure hospitalizations and mortality in France, Circulation 100 (1999) 280–286.
[2] J.R. Allegra, D.G. Cochrane, R. Biglow, Monthly, weekly, and daily patterns in the incidence of congestive heart failure, Acad. Emerg. Med. 8 (2001) 682–685.
[3] S. Stewart, K. McIntyre, S. Capewell, J.J. McMurray, Heart failure in a cold climate. Seasonal variation in heart failure-related morbidity and mortality, J. Am. Coll. Cardiol. 39 (2002) 760–766.
[4] A. Diaz, D. Ferrante, R. Badra, I. Morales, A. Becerra, S. Varini, D. Nul, H. Grancelli, H. Doval, Seasonal variation and trends in heart failure morbidity and mortality in a South American community hospital, Congest. Heart Fail. 13 (2007) 263–266.
[5] M. Ogawa, F. Tanaka, T. Onoda, M. Ohsawa, K. Itai, T. Sakai, A. Okayama, M. Nakamura, A community based epidemiological and clinical study of hospitalization of patients with congestive heart failure in Northern Iwate, Japan, Circ. J. 71 (2007) 455–459.
[6] V.O. Ansa, J.U. Ekott, I.O. Essien, E.O. Bassey, Seasonal variation in admission for heart failure, hypertension and stroke in Uyo, South-Eastern Nigeria, Ann. Afr. Med. 7 (2008) 62–66.
[7] J.I. Halonen, A. Zanobetti, D. Sparrow, P.S. Vokonas, J. Schwartz, Relationship between outdoor temperature and blood pressure, Occup. Environ. Med. 68 (2011) 296–301.
[8] P.T. Wilmshurst, M. Nuri, A. Crowther, M.M. Webb-Peploe, Cold-induced pulmonary oedema in scuba divers and swimmers and subsequent development of hypertension, Lancet 1 (1989) 62–65.
[9] M.J. Caterina, M.A. Schumacher, M. Tominaga, T.A. Rosen, J.D. Levine, D. Julius, The capsaicin receptor: a heat-activated ion channel in the pain pathway, Nature 389 (1997) 816–824.
[10] M.J. Caterina, T.A. Rosen, M. Tominaga, A.J. Brake, D. Julius, A capsaicin-receptor homologue with a high threshold for noxious heat, Nature 398 (1999) 436–441.
[11] E. Mezey, Z.E. Toth, D.N. Cortright, M.K. Arzubi, J.E. Krause, R. Elde, A. Guo, P.M. Blumberg, A. Szallasi, Distribution of mRNA for vanilloid receptor subtype 1 (VR1), and VR1-like immunoreactivity, in the central nervous system of the rat and human, Proc. Natl. Acad. Sci. USA 97 (2000) 3655–3660.
[12] J.C. Roberts, J.B. Davis, C.D. Benham, [3H]Resiniferatoxin autoradiography in the CNS of wild-type and TRPV1 null mice defines TRPV1 (VR-1) protein distribution, Brain Res. 995 (2004) 176–183.
[13] M.D. Southall, T. Li, L.S. Gharibova, Y. Pei, G.D. Nicol, J.B. Travers, Activation of epidermal vanilloid receptor-1 induces release of proinflammatory mediators in human keratinocytes, J. Pharmacol. Exp. Ther. 304 (2003) 217–222.
[14] L.R. Sadofsky, R. Ramachandran, C. Crow, M. Cowen, S.J. Compton, A.H. Morice, Inflammatory stimuli up-regulate transient receptor potential vanilloid-1 expression in human bronchial fibroblasts, Exp. Lung Res. 38 (2012) 75–81.
[15] L. Ma, J. Zhong, Z. Zhao, Z. Luo, S. Ma, J. Sun, H. He, T. Zhu, D. Liu, Z. Zhu, M. Tepel, Activation of TRPV1 reduces vascular lipid accumulation and attenuates atherosclerosis, Cardiovasc. Res. 92 (2011) 504–513.
[16] C.L. Buckley, A.J. Stokes, Mice lacking functional TRPV1 are protected from pressure overload cardiac hypertrophy, Channels (Austin) 5 (2011) 367–374.
[17] M.R. Zahner, D.P. Li, S.R. Chen, H.L. Pan, Cardiac vanilloid receptor 1-expressing afferent nerves and their role in the cardiogenic sympathetic reflex in rats, J. Physiol. 551 (2003) 515–523.
[18] L. Wang, D.H. Wang, TRPV1 gene knockout impairs postischemic recovery in isolated perfused heart in mice, Circulation 112 (2005) 3617–3623.
[19] J. Peng, Y.J. Li, The vanilloid receptor TRPV1: role in cardiovascular and gastrointestinal protection, Eur. J. Pharmacol. 627 (2010) 1–7.

[20] F. Thilo, Y. Liu, N. Schulz, U. Gergs, J. Neumann, C. Loddenkemper, M. Gollasch, M. Tepel, Increased transient receptor potential vanilloid type 1 (TRPV1) channel expression in hypertrophic heart, Biochem. Biophys. Res. Commun. 401 (2010) 98–103.

[21] J.S. Horton, C.L. Buckley, A.J. Stokes, Successful TRPV1 antagonist treatment for cardiac hypertrophy and heart failure in mice, Channels (Austin) 7 (2013) 17–22.

[22] V. Farfariello, C. Amantini, G. Santoni, Transient receptor potential vanilloid 1 activation induces autophagy in thymocytes through ROS-regulated AMPK and Atg4C pathways, J. Leukoc. Biol. 92 (2012) 421–431.

[23] D.F. Dai, P. Rabinovitch, Mitochondrial oxidative stress mediates induction of autophagy and hypertrophy in angiotensin-II treated mouse hearts, Autophagy 7 (2011) 917–918.

[24] A.P. Rogerio, E.L. Andrade, J.B. Calixto, C-fibers, but not the transient potential receptor vanilloid 1 (TRPV1), play a role in experimental allergic airway inflammation, Eur. J. Pharmacol. 662 (2011) 55–62.

[25] N. Clark, J. Keeble, E.S. Fernandes, A. Starr, L. Liang, D. Sugden, P. de Winter, S.D. Brain, The transient receptor potential vanilloid 1 (TRPV1) receptor protects against the onset of sepsis after endotoxin, FASEB J 21 (2007) 3747–3755.

[26] T.A. Doser, S. Turdi, D.P. Thomas, P.N. Epstein, S.Y. Li, J. Ren, Transgenic overexpression of aldehyde dehydrogenase-2 rescues chronic alcohol intake-induced myocardial hypertrophy and contractile dysfunction, Circulation 119 (2009) 1941–1949.

[27] A.F. Ceylan-Isik, P. Zhao, B. Zhang, X. Xiao, G. Su, J. Ren, Cardiac overexpression of metallothionein rescues cardiac contractile dysfunction and endoplasmic reticulum stress but not autophagy in sepsis, J. Mol. Cell Cardiol. 48 (2010) 367–378.

[28] S. Turdi, M.R. Kandadi, J. Zhao, A.F. Huff, M. Du, J. Ren, Deficiency in AMP-activated protein kinase exaggerates high fat diet-induced cardiac hypertrophy and contractile dysfunction, J. Mol. Cell Cardiol. 50 (2011) 712–722.

[29] H. Ma, S.Y. Li, P. Xu, S.A. Babcock, E.K. Dolence, M. Brownlee, J. Li, J. Ren, Advanced glycation endproduct (AGE) accumulation and AGE receptor (RAGE) up-regulation contribute to the onset of diabetic cardiomyopathy, J. Cell Mol. Med. 13 (2009) 1751–1764.

[30] M. Dong, N. Hu, Y. Hua, X. Xu, M.R. Kandadi, R. Guo, S. Jiang, S. Nair, D. Hu, J. Ren, Chronic Akt activation attenuated lipopolysaccharide-induced cardiac dysfunction via Akt/GSK3beta-dependent inhibition of apoptosis and ER stress, Biochim. Biophys. Acta. 2013 (1832) 848–863.

[31] Y. Zhang, N. Hu, Y. Hua, K.L. Richmond, F. Dong, J. Ren, Cardiac overexpression of metallothionein rescues cold exposure-induced myocardial contractile dysfunction through attenuation of cardiac fibrosis despite cardiomyocyte mechanical anomalies, Free Radic. Biol. Med. 53 (2012) 194–207.

[32] F. Thilo, Y. Liu, N. Schulz, U. Gergs, J. Neumann, C. Loddenkemper, M. Gollasch, M. Tepel, Increased transient receptor potential vanilloid type 1 (TRPV1) channel expression in hypertrophic heart, Biochem. Biophys. Res. Commun. 401 (2010) 98–103.

[33] M. Juhaszova, D.B. Zorov, S.H. Kim, S. Pepe, Q. Fu, K.W. Fishbein, B.D. Ziman, S. Wang, K. Ytrehus, C.L. Antos, E.N. Olson, S.J. Sollott, Glycogen synthase kinase-3beta mediates convergence of protection signaling to inhibit the mitochondrial permeability transition pore, J. Clin. Invest. 113 (2004) 1535–1549.

[34] M.H. Rider, N. Hussain, S. Horman, S.M. Dilworth, K.B. Storey, Stress-induced activation of the AMP-activated protein kinase in the freeze-tolerant frog Rana sylvatica, Cryobiology 53 (2006) 297–309.